the plant journal

SEB SOCIETY FOR EXPERIMENTAL BIOLOGY

The Plant Journal (2020) doi: 10.1111/tpj.15052

Expression dynamics of dehydration tolerance in the tropical plant *Marchantia inflexa*

Rose A. Marks[1,2,3*], Jeramiah J. Smith[1], Robert VanBuren[2,3] and David Nicholas McLetchie[1]

[1]*Department of Biology, University of Kentucky, Lexington, KY 40506, USA,*

[2]*Department of Horticulture, Michigan State University, East Lansing, MI 48824, USA, and*

[3]*Plant Resilience Institute, Michigan State University, East Lansing, MI 48824, USA*

Received 6 December 2019; revised 10 September 2020; accepted 24 September 2020.

*For correspondence (e-mail marksros@msu.edu).

SUMMARY

Tolerance to prolonged water deficit occurs along a continuum in plants, with dehydration tolerance (DhT) and desiccation tolerance (DT) representing some of the most extreme adaptations to water scarcity. Although DhT and DT presumably vary among individuals of a single species, this variability remains largely unstudied. Here, we characterized expression dynamics throughout a dehydration–rehydration time-course in six diverse genotypes of the dioecious liverwort *Marchantia inflexa*. We identified classical signatures of stress response in *M. inflexa*, including major changes in transcripts related to metabolism, expression of LEA and ELIP genes, and evidence of cell wall remodeling. However, we detected very little temporal synchronization of these responses across different genotypes of *M. inflexa*, which may be related to genotypic variation among samples, constitutive expression of dehydration-associated transcripts, the sequestration of mRNAs in ribonucleoprotein partials prior to drying, or the lower tolerance of *M. inflexa* relative to most bryophytes studied to date. Our characterization of intraspecific variation in expression dynamics suggests that differences in the timing of transcriptional adjustments contribute to variation among genotypes, and that developmental differences impact the relative tolerance of meristematic and differentiated tissues. This work highlights the complexity and variability of water stress tolerance, and underscores the need for comparative studies that seek to characterize variation in DT and DhT.

Keywords: drought, dehydration tolerance, desiccation tolerance, expression dynamics, transcriptome, genetic variation, sex, liverwort, *Marchantia inflexa*.

INTRODUCTION

The ability of plants to tolerate abiotic stress has important implications for ecosystem function, plant community dynamics and agricultural productivity (Lesk *et al.*, 2016). In order to improve food security and mitigate economic losses due to changing environmental conditions, a comprehensive understanding of the physiology and evolution of abiotic stress tolerance in plants is needed. Drought, in particular, is a major threat to agricultural productivity (Lesk *et al.*, 2016), and is predicted to increase in the coming years in many of the food-producing regions of the world (Trenberth, 2011; Dai, 2013). Consequently, there is an urgent need to characterize the physiological, biochemical and genetic mechanisms of drought tolerance in order to optimize agricultural production, secure plant-based industries and improve natural resource management.

Desiccation tolerance (DT, also desiccation tolerant) is an extreme form of water stress tolerance with promising translational applications. Most plants are desiccation sensitive (DS) and cannot survive drying below −5 to −10 MPa (Proctor and Pence, 2002; Proctor *et al.*, 2007; Oliver *et al.*, 2010), but DT plants recover after drying to or below an absolute water content of −100 MPa (Alpert and Oliver, 2002). Dehydration tolerance (DhT, also dehydration tolerant) is a less extreme version of water stress tolerance. DhT plants can survive drying to < -10 MPa, but not < -100 MPa (Oliver *et al.*, 2010; Marks *et al.*, 2016). Although DT has been relatively well studied, few studies on DhT exist. DT is a complex trait, dependent on the synchronized orchestration of multiple physiological and molecular processes, but how DhT compares with DT is not well known. Enhanced understanding of both DT and DhT will facilitate progress towards applied objectives.

On a cellular level, dehydration causes both mechanical and oxidative stress. Cytoplasmic shrinkage during dehydration and subsequent expansion upon rehydration place considerable mechanical strain on cell walls, membranes

and macromolecules. Consequently, many DT plants have flexible cell walls that can accommodate large changes in volume (Platt *et al.*, 1997; Vicré *et al.*, 2004; Moore *et al.*, 2008). Modifications in carbohydrate metabolism leading to the accumulation of small, non-reducing sugars and other osmoprotectants are another important mechanism of stabilizing membranes and macromolecules during drying via vitrification (Smirnoff, 1992; Illing *et al.*, 2005; Dinakar *et al.*, 2012). In addition to the mechanical strain imposed during dehydration, oxidative stress is another major source of damage under dehydrated conditions (Scheibe and Beck, 2011). The formation of reactive oxygen species (ROS) is inevitable even under non-stressed conditions (Choudhury *et al.*, 2017), and subtle changes in ROS production can even act as an initial signal of stress (Choudhury *et al.*, 2017). However, dehydration can increase ROS production to potentially damaging levels due to the disruption of cellular homeostasis and resulting build-up of reactive metabolic intermediates, particularly in photosynthetic tissues (Dinakar *et al.*, 2012; Sharma *et al.*, 2012). Consequently, DT plants have evolved diverse mechanisms to minimize damage from ROS, including the rapid termination of photosynthetic processes, changes in metabolic flux, and the synthesis and mobilization of protective pigments, enzymatic and non-enzymatic antioxidants (Dinakar *et al.*, 2012). Two groups of proteins [late embryogenesis abundant (LEA) proteins and early light inducible proteins (ELIPs)] have received considerable attention due to their putative roles in minimizing both mechanical and oxidative stress during dehydration. LEAs are thought to stabilize membranes, subcellular organization and facilitate protein folding via chaperone activity (Bremer *et al.*, 2017; Costa *et al.*, 2017; Artur *et al.*, 2019). ELIPs appear to prevent photooxidative damage by stabilizing the photosynthetic apparatus via chlorophyll binding (Zeng *et al.*, 2002; Vanburen *et al.*, 2019). Recent evidence shows that ELIP genes have undergone considerable expansion in DT lineages relative to DS lineages, suggesting a central role for ELIPs in DT and possibly DhT (Vanburen *et al.*, 2019).

In addition to being complex, DT and DhT vary across and within species, which presents a significant challenge to accurately identifying tolerance mechanisms (Oliver *et al.*, 2020). Although some core mechanistic elements appear to be shared across organisms (Crowe *et al.*, 1998; Alpert, 2005), substantial variation in phenotypes is also evident across diverse lineages (Oliver *et al.*, 1993; Farrant, 2000), populations of the same species (Marks *et al.*, 2019a) and developmental stages of a single plant (Greenwood *et al.*, 2019; Radermacher *et al.*, 2019). Major differences have been identified among vascular and non-vascular DT plants. Most vascular plants mobilize stress responses at the onset of drying, but many bryophytes appear to constitutively express and sequester mRNAs in ribonucleoprotein particles for rapid mobilization during drying (Wood and Oliver, 1999; Oliver *et al.*, 2000). Variation in photosynthetic responses (Tuba *et al.*, 1998; Farrant, 2000), osmoprotectant composition (Ghasempour *et al.*, 1998) and antioxidant responses (Farrant, 2000) is also evident across DT lineages. Intraspecific variability in DT and DhT is less well understood, but is essential for adaptation to changing environments. Characterizing the extent of intraspecific variability in DT and DhT will aid in untangling the complex interactions of genotype by environment and enhance predictions of possible species range shifts.

In order to pinpoint characteristics that increase water stress tolerance, comparative analyses are needed on multiple levels. Initially, the different degrees of tolerance ranging from DS to DT must be carefully defined, and the progressive changes in physiology, biochemistry and genetics along this spectrum should be catalogued. Although studies comparing DS with DT plants exist (Vander Willigen *et al.*, 2001; Oliver *et al.*, 2011; VanBuren *et al.*, 2018), less is known about the molecular biology of plants with intermediate water stress responses (i.e. DhT plants). Careful characterization of the ecological, physiological and molecular characteristics of DhT plants will provide important insights into the progressive differences between DT and DS plants, which can be used to refine targets for crop improvement. In addition, the degree and patterns of intraspecific variation in water stress tolerance should be characterized. The limited studies on intraspecific variation in DT and DhT suggest that considerable variation exists (Farrant and Kruger, 2001; Stark *et al.*, 2007; Farrant *et al.*, 2009; Marks *et al.*, 2016), but the underlying mechanism driving this variation is not known. Studies of intraspecific variation can be used to identify exceptionally tolerant eco- and genotypes, and to test if phenotypic variation derives from plasticity or genetic differences. Finally, studies addressing the causes and consequences of sexual dimorphisms in DT and DhT are needed. Understanding sexual dimorphisms in stress tolerance is critical because these dimorphisms can drive spatial segregation of the sexes, biased population sex ratios, and may ultimately reduce sexual reproduction and population persistence for dioecious plants (Juvany and Munné-Bosch, 2015).

In an effort to fill gaps in our understanding of water stress responses, we characterized the expression dynamics during a dehydration–rehydration time-course in a highly variable and dioecious DhT plant. *Marchantia inflexa* (Nees & Mont) is a tropical liverwort that is distributed from northern Venezuela to the southern USA (Bischler, 1984), and exhibits substantial intraspecific variation in DhT (Marks *et al.*, 2016, 2019a). Here, we sequenced two distinct tissue types (meristematic and differentiated thallus) in six diverse genotypes from a single population of *M. inflexa* to gain insight into the molecular mechanisms underlying intraspecific variability in DhT. Because

there is a sex difference in DhT within the source population, the three most DhT genotypes were females and the three least DhT genotypes were male, which provided an opportunity to link our findings to the previously characterized sexual dimorphism in DhT. Analyses of global gene expression revealed signatures of stress response in *M. inflexa*. However, we also detected a general disorganization in the response of *M. inflexa* to dehydration, providing a possible explanation for the decreased tolerance of *M. inflexa* relative to highly DT plants.

RESULTS

Dehydration treatment and verification of recovery

Plants were subjected to dehydration treatment as described in Marks *et al.* (2016) and sampled at five predetermined time-points during the dehydration–rehydration process: fully hydrated (baseline); partially dehydrated at 15 h (Dh15); dehydrated at 22 h (Dh22); 2 h after rehydration (Rh2); and 24 h after rehydration (Rh24; Figure S1). Samples showed visual signs of drying at Dh15 (characterized by a rubbery texture) and were dehydrated at Dh22 (characterized by substantial shrinkage and thallus curling). These morphological changes are characteristic of predictable relative water contents experienced throughout dehydration treatment.

To verify that dehydration assays were performing as expected, sample recovery was quantified by measuring chlorophyll fluorescence 2 weeks after rehydration (when plants were expected to be fully recovered). All evaluated samples recovered from dehydration treatment. After 2 weeks in recovery conditions, mean F_v/F_m was 0.72 ± 0.03 with no significant differences between genotypes (Figure S2). In addition, the special distribution of tissue recovery was estimated on the basis of green versus brown tissues. Visually, tissue recovery ranged from 1.5% to 97.8% survival, but in all instances the meristematic region was among the recovered portion of the sample. Tissue death became increasingly likely as distance from the meristem increased, with the most distal region recovering only 6% of the samples.

Relationship between DhT genotypes

To estimate relatedness among *M. inflexa* genotypes, we computed the pairwise genetic distance between isolates based on 21 394 binary variants. We detected moderate genetic variation among the six genotypes, which may contribute to relative differences in DhT (Figure S3).

In total, 60 RNAseq libraries were sequenced from meristematic and differentiated tissues of six genotypes at five hydration states, collectively spanning ~1.3 billion reads. Using the *M. inflexa* draft genome (Marks *et al.*, 2019b) as a guide, we assembled a *M. inflexa* transcriptome consisting of 26 977 transcripts across 21 704 334 assembled bases with an N50 of 1039. Assessment of transcriptome completeness indicated that 58.5% of the expected Universal Single-copy Orthologs were present in our assembly (34.7% complete, and 23.8% fragmented). This relatively low number may reflect inherent limitations of applying BUSCO to deeply diverged lineages as has been noted in previous studies involving *Marchantia* and other early diverging lineages (Smith *et al.*, 2018; Marks *et al.*, 2019b). Alternatively, because we did not sample a comprehensive panel of developmental stages and tissues (i.e. sporophyte, reproductive tissues and gemmae), this transcriptome may not capture the full suite of *M. inflexa* genes.

Functional annotation with Trinotate identified homologs for 21 501 of the 26 977 *M. inflexa* transcripts (79.7%) across UniProtKB/Swiss-Prot, *Arabidopsis thaliana*, *Physcomitrella patens* and *Marchantia polymorpha*. The 5476 transcripts with no known homology were classified as 'homolog not identified'. Of the transcripts with homology, gene ontology (GO) terms were assigned to 16 309. The remaining 5192 transcripts were classified as 'GO function not assigned'. The most common biological processes in the *M. inflexa* dehydration–rehydration transcriptome were regulation of transcription, carbohydrate metabolism, cell cycle and multicellular organism development. Additional GO terms related to DhT were detected, including cellular response to desiccation, lipid transport and metabolism, protein ubiquitination, and heat acclimation. The most abundant protein classes represented in the *M. inflexa* transcriptome were nucleic acid binding, hydrolase, transferase, oxidoreductase and transporter classes.

Expression dynamics during dehydration and rehydration

To summarize the relationship among tissue, genotype and time-point, we conducted a principal component analysis (PCA) of global gene expression. Principal components 1 and 2 of the PCA accounted for 68.15% (66.35 and 1.80%, respectively) of the total variance in gene expression (Figure 1). PC1 explained by far the highest proposition of the variability in gene expression, and the majority of genes had negative loading scores on PC1, reflective of a broad downregulation of gene expression during dehydration. There were 13 414 genes with loading scores < -1 on PC1, and these were functionally enriched for GO terms related to translation ($P = 5.5e\text{-}16$), response to cadmium ion ($P = 4.9e\text{-}14$), response to cytokinin ($P = 3.9e\text{-}10$), mRNA processing ($P = 2.7e\text{-}9$) and protein transport ($P = 2.6e\text{-}8$). Fewer transcripts had positive loading scores on PC1, but the 555 transcripts with scores > 1 were functionally enriched for GO terms related to protein-chromophore linkage ($P = 0.0001$), endosome to vacuole transport ($P = 0.0001$), vacuole ($P = 0.00089$) and amyloplast ($P = 0.0032$) organization, and photosynthesis ($P = 0.0004$). Genes that had no (or very low) loading

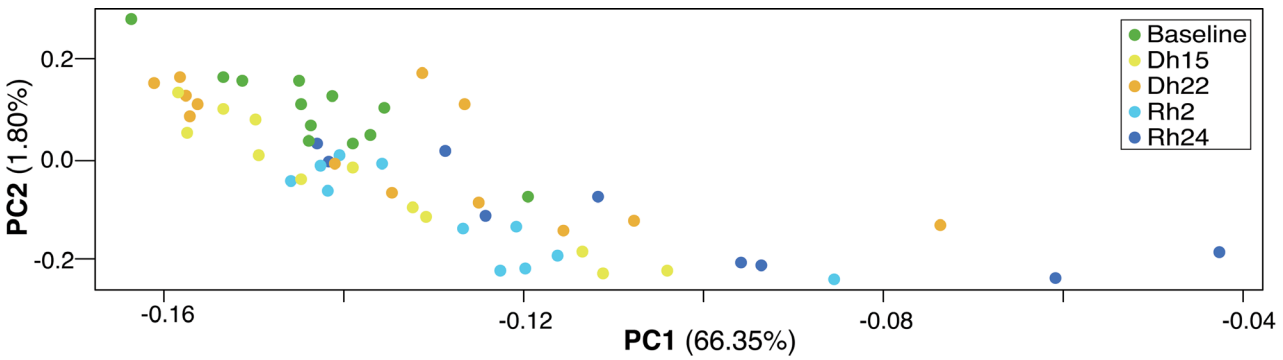

Figure 1. Principal component analyses (PCAs) of global gene expression.
The hydration status of samples is represented by color. Negligible differentiation among samples was evident along additional PCs. There were weak patterns of association among the sexes and tissues (not shown).

scores on PC1 were enriched for GO terms related to N-glycan processing (P = 4.2e-5), acyl-chain remodeling (P = 0.004) and regulation of mitochondrial membrane permeability (P = 0.002). Samples from different genotypes, tissues and hydration states were broadly interspersed along PC1. Baseline samples exhibited similar gene expression patterns to one another, but other hydration states were less distinct. Additional PCs explained decreasing proportions of the variance in gene expression and did not provide further insight into sample relationships. There were no obvious patterns of association among the sexes and tissues. PCA of individual genotypes revealed highly variable expression across genotypes (Figure S4), suggesting that genotypic variation may contribute to the inconsistency in gene expression patterns observed.

To investigate temporal changes in gene expression during the dehydration–rehydration time-course, we identified genes that were significantly up- or downregulated at each time-point relative to baseline conditions. From these analyses we defined a list of 619 non-redundant differentially expressed genes [DEGs; false discovery rate (FDR) $P < 0.05$]. Two-way clustering of these DEGs revealed complex and variable relationships among samples and genes (Figure 2). DEGs were clustered into seven semi-distinct groups based on similarity in expression patterns. Clusters 1–4 exhibited erratic expression across time, and were enriched for GO terms related to jasmonic acid signaling (P = 0.0009), protein deubiquitination (P = 0.0009), acetyl-CoA biosynthesis (P = 0.0002), ribonucleoprotein complex assembly (P = 0.0027) and leaf senescence (P = 0.0009). Cluster 5 genes exhibited dehydration-induced increases in expression that persisted into rehydration, and were enriched for GO terms related to the negative regulation of DNA-templated transcription (P = 0.001), response to water deprivation (P = 0.0096) and cold acclimation (P = 0.017). Cluster 6 genes exhibit distinct increases in expression during early rehydration, and were enriched for GO terms related to mitochondrial electron transport (P = 0.0009), negative regulation of cytokinin activated signaling (P = 0.0018) and photosynthesis (P = 0.01). Cluster 7 contained genes that were sporadically downregulated during both dehydration and rehydration, and were enriched for GO terms related to copper ion transport (P = 0.0008) and isopentenyl diphosphate biosynthesis (P = 0.0003). Similar to the PCA, baseline samples exhibited the most consistent gene expression patterns across genotypes, whereas expression profiles of plants at Dh15, Dh22, Rh2 and Rh24 were less distinct (Figure 2).

The majority of DEGs (66%) were downregulated at one or more time-points, and 15% were downregulated across all time-points. In contrast, only 34% of DEGs were upregulated at one or more time-point, and half of these were uniquely upregulated at Rh24 but showed no differential expression at any other time-point. We identified a small set of genes (1%) that were consistently upregulated throughout the entire time-course (Figure 3). We summarized the functional role of these gene sets via GO enrichment analyses. In general, GO terms enriched in downregulated genes were related to transpiration (P = 0.0004), nuclear polyadenylation-dependent mRNA catabolic processes (P = 0.0004), ribonucleoprotein complex assembly (P = 0.004) and copper ion transport (P = 0.004). In contrast, upregulated genes were enriched for GO terms related to diaminopimelate biosynthesis (P = 0.0022), hydrogen peroxide catabolism (P = 0.0254) and rRNA processing (P = 0.0471; Figure 4).

The LEA and ELIP gene families have well-characterized roles in DT with universal upregulation during dehydration. We identified 39 *M. inflexa* LEA orthologs and seven ELIP orthologs with a cumulative TMM > 10. Many *M. inflexa* LEAs exhibited inconsistent expression across time-points. However, some dehydrins (particularly 1, 3, 5, 13 and 16) and LEA4 family proteins showed dehydration-responsive expression (with some genotypic variation). LEA2-1, 4 and 14 exhibited constitutive expression. ELIPs 5 and 7 were most highly expressed throughout the

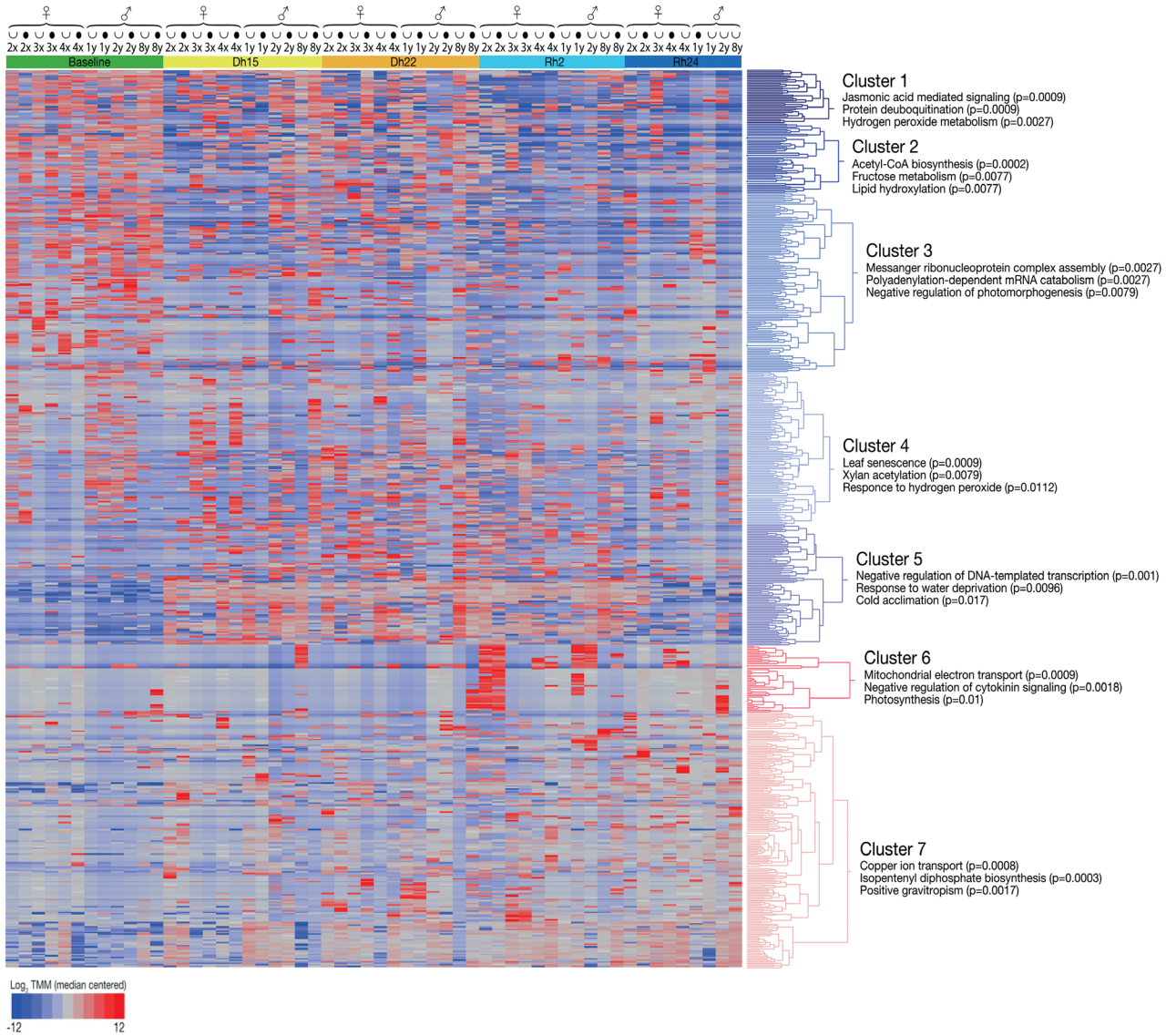

Figure 2. Hierarchal clustering of 619 non-redundant dehydration–rehydration responsive genes [false discovery rate (FDR) $P < 0.05$].
Gene expression values (TMM) were $\log_2$-transformed and median-centered prior to clustering. Each column represents a single sample, and each row represents a single transcript. Red indicates higher expression and blue indicates lower expression. Hierarchal gene relationships are shown on the right *y*-axis. Seven clusters of genes are defined, and the most enriched gene ontology (GO) terms for each cluster are listed. Colored boxes designate hydration state, female (♀) and male (♂) symbols designate sample sex, meristematic (•) and differentiated (U) symbols designate tissue type, and genotype names are given.

dehydration–rehydration process, but patterns across genotypes and tissues were irregular (Figure 5).

Differences in gene expression among the genotypes and tissues

Broadly, we identified very little overlap between high DhT (female) and low DhT (male) DEGs. Consistent with overall patterns, the majority of DEGs were downregulated in both groups. Both males and females had more DEGs (up- and downregulated) during rehydration (Figure 6). We summarized the function of these sexually dimorphic genes sets via GO analysis. During dehydration, females exhibited increased expression of genes related to glycoprotein catabolism ($P = 0.0027$), and decreased expression of starch ($P = 0.0026$) and amylopectin ($P = 0.0117$) biosynthesis genes. Males, on the other hand, showed increased expression of genes-related transcription ($P = 0.0055$) and rRNA processing ($P = 0.0471$), but decreased expression of genes related to transpiration ($P = 0.0059$) and hydrogen peroxide transport ($P = 0.0059$). During rehydration, females increased expression of hydrogen peroxide ($P = 0.0016$) and auxin ($P = 0.0016$) catabolism and decreased expression genes related to the glyoxylate cycle ($P = 0.0019$) and the negative regulation of apoptosis

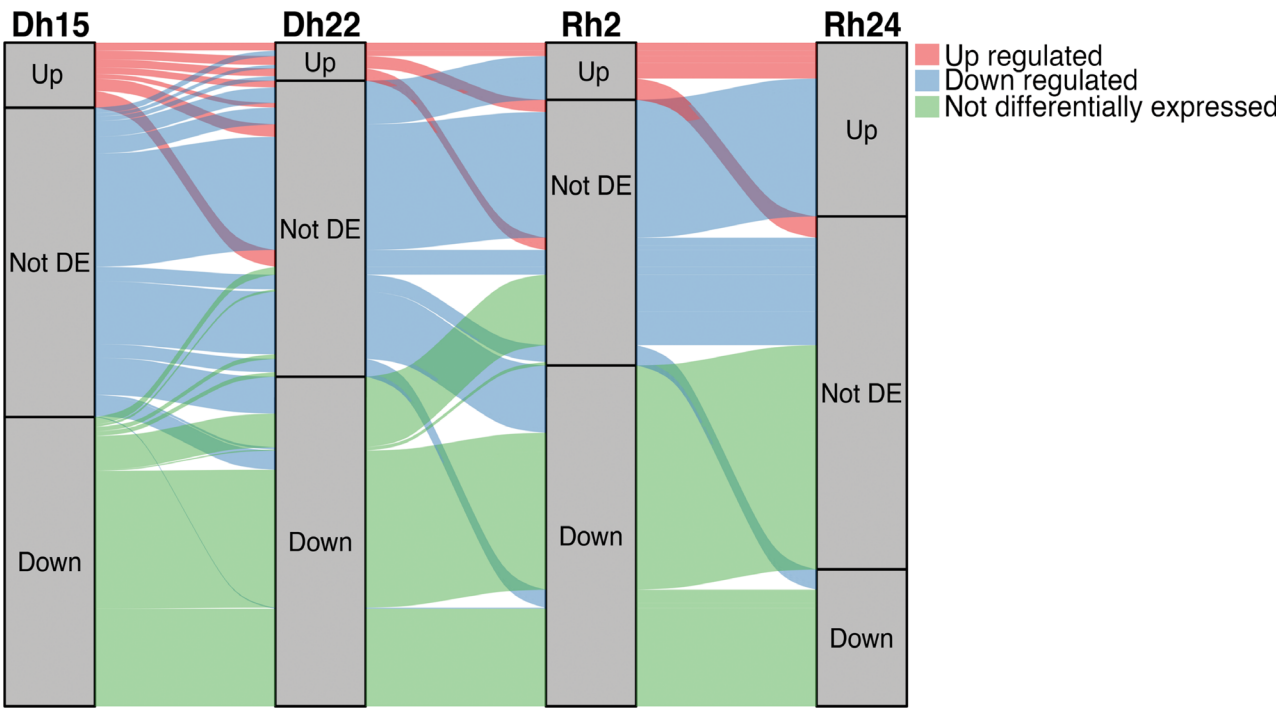

Figure 3. Alluvial diagram showing expression patterns across time of hydration-responsive differentially expressed genes (DEGs) with false discovery rate (FDR) $P < 0.05$.
Each transcript was designated as either upregulated (up), downregulated (down), or not differentially expressed (not DE) for each time-point. Flows between time-points follow specific genes sets. Colors represent the expression status of that gene set at the last time-point.

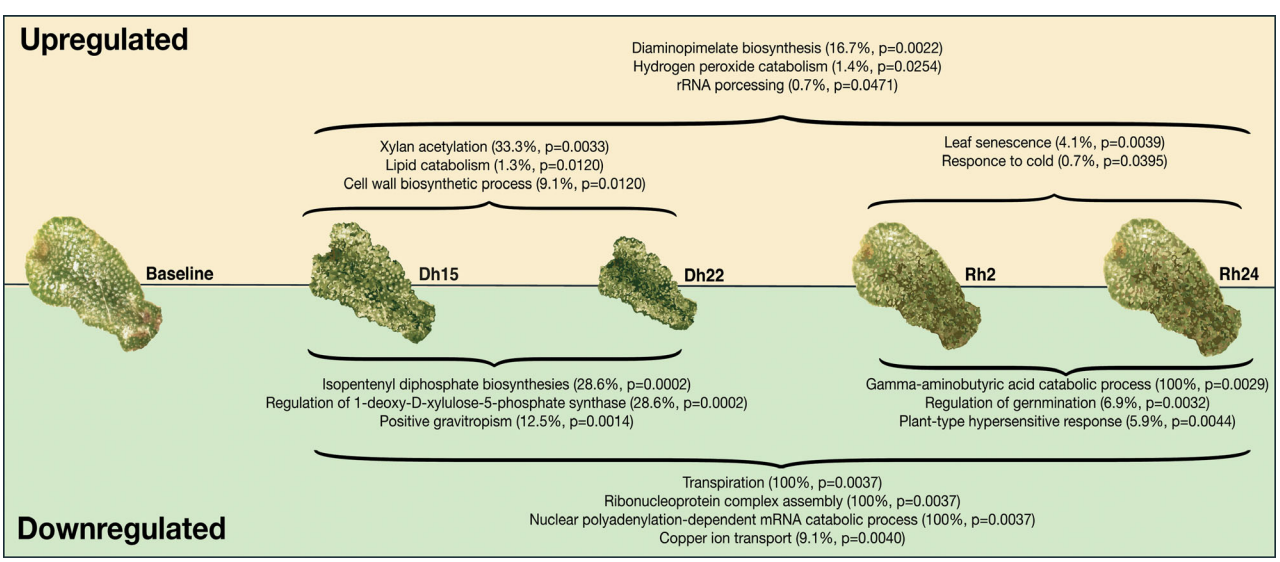

Figure 4. Summary of dehydration tolerance (DhT) responses in *Marchantia inflexa* throughout the dehydration–rehydration time-course. Enriched gene ontology (GO) terms were identified for both up- and downregulated genes throughout the time-course. From these analyses, we generated a generalized model of temporal DhT responses in *M. inflexa*. GO terms that were enriched in upregulated genes are shown in the upper portion of the figure, and GO terms enriched in downregulated genes are shown in the lower half of the figure. The percentage of genes for each GO term that were differentially expressed and the statistical significance of enrichment is given.

($P = 0.0041$), whereas males increased expression of genes involved in sugar metabolism and decreased expression of genes involved in photosynthetic processes (Figure 7).

Very few DEGs were shared between meristematic and differentiated tissues. Meristematic tissues were characterized by numerous changes in expression during

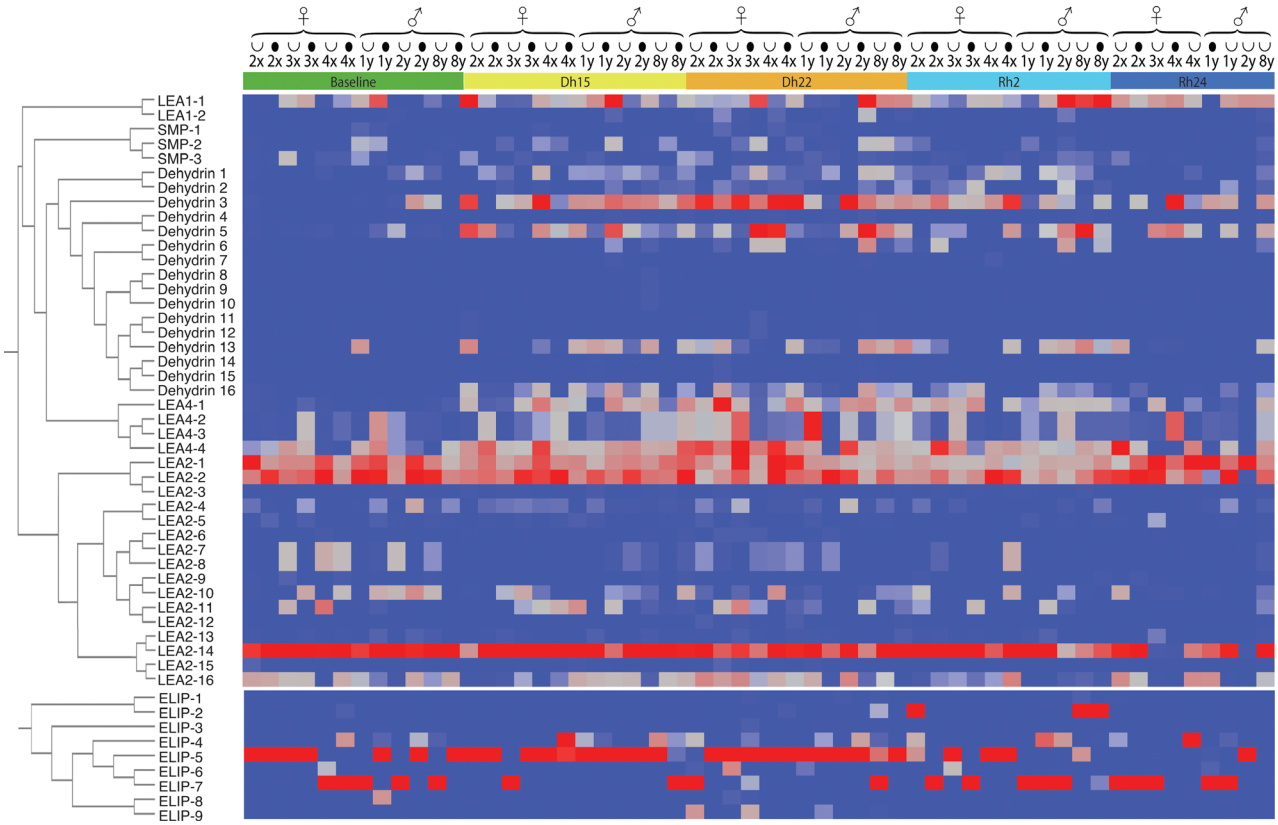

Figure 5. Heatmap of late embryogenesis abundant (LEA) and early light inducible protein (ELIP) expression values (TMM) across time.
Red indicates higher expression and blue represents lower expression. Gene relatedness was determined through analyses of sequence similarity. Gene relationships for *Marchantia inflexa* LEA and ELIP are visualized with cladograms on the *y*-axis. Samples are ordered by time, sex and genotype. Colored boxes designate hydration state, female (♀) and male (♂) symbols designate sample sex, meristematic (•) and differentiated (U) symbols designate tissue type, and genotype names are given.

dehydration and early rehydration, whereas differentiated tissues exhibited more numerous changes in gene expression during rehydration (Figure 8). During dehydration, meristematic tissues showed increased expression of genes related to intracellular transport ($P = 0.0073$), jasmonic acid signaling ($P = 0.0353$) and translation ($P = 0.0203$), but decreased expression of genes involved in transpiration ($P = 0.0003$). Differentiated tissues showed increased expression of a single gene involved in xyloglucan biosynthesis ($P = 0.0024$) and decreased expression of genes related to cellular differentiation during dehydration. During rehydration, meristematic tissues exhibited increased expression of carbohydrate biosynthetic and metabolic processing genes and chromatin silencing genes ($P = 0.0084$), but decreased expression of lipid metabolic processing genes. In comparison, differentiated tissues showed increased expression of genes involved in photosystem II (PSII) assembly ($P = 0.0004$) and decreased expression of genes involved in transpiration ($P = 0.0003$; Figure 7).

DISCUSSION

Our characterization of the *M. inflexa* dehydration–rehydration transcriptome revealed extensive and complex patterns of intraspecific variation in gene expression. We identified common signatures of stress response in *M. inflexa*, including substantial changes in the expression of transcripts related to ROS scavenging, carbohydrate metabolism and protein ubiquitination, all of which are broadly implicated in DT (Dinakar *et al.*, 2012; Lin *et al.*, 2019). This suggests that *M. inflexa* responds to dehydration by leveraging some of the same central mechanisms observed in highly DT lineages. However, many of these are common responses that are also shared with DS plants (Pardo *et al.*, 2020). We also noted potentially important differences between *M. inflexa* and highly DT plants, the most obvious of which was a general disorganization of temporal responses and lack of consistency across genotypes. Comparisons among diverse genotypes [high DhT (female) versus low DhT (male)] and tissues (meristematic versus differentiated tissues) allowed us to target nuanced variation in gene expression that may contribute to differences in survival outcomes.

Most DT plants exhibit a characteristic suite of responses to drying, including anatomical and morphological modifications (e.g. leaf folding and pigmentation changes); a coordinated shutdown of photosynthetic processes during

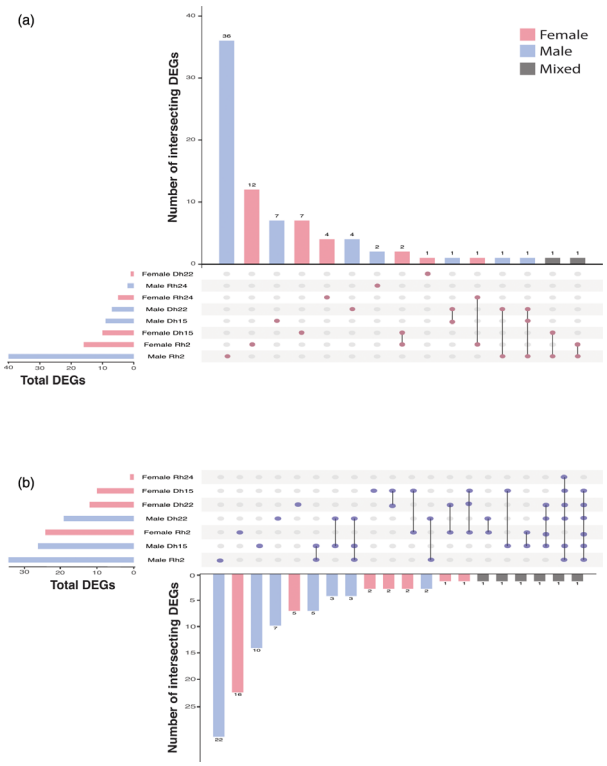

Figure 6. Upset plots showing the number of differentially expressed genes (DEGs) in each sex and time-point for upregulated genes (a) and downregulated genes (b).
DEGs [false discovery rate (FDR) < 0.05] were identified by comparing gene expression at experimental time-points with gene expression at baseline to generate a sex- and time-specific gene set. The total number of DEGs identified for each gene set is listed on the side bar plot, and the number of unique and common (non-overlapping and overlapping) genes are displayed in the main histogram. A colored circle indicates the gene set. Colored circles connected by a line indicate common (overlapping) gene sets. A gray circle indicates that the gene set is absent in that sample. There were no male DEGs at Rh24. Bar color indicates sex.

drying (Dinakar *et al.*, 2012); increased cell wall flexibility to alleviate the mechanical stress of shrinkage (Farrant, 2000; Moore *et al.*, 2006); modified carbohydrate metabolism leading to the accumulation of small non-reducing sugars (Smirnoff, 1992); increased production of various stress-related proteins including ELIPs and LEAs (Costa *et al.*, 2017; Vanburen *et al.*, 2019); increased antioxidant activity related to ROS scavenging (Dinakar and Bartels, 2013); and abscisic acid mediated and phospholipid signaling (Dinakar *et al.*, 2012). Our work indicates that some of these same processes are induced in *M. inflexa* during drying. We detected changes in carbohydrate metabolism, a persistent response to oxidative stress, and modifications to cell wall biochemistry in dehydrating *M. inflexa* samples. Current models of DT suggest that LEAs and ELIPs play a central role in water stress responses in DT plants (Liu *et al.*, 2009; Dinakar *et al.*, 2012; Costa *et al.*, 2017), and we identified expression of putative LEAs and ELIPs throughout the dehydration–rehydration time-course in *M. inflexa*. Finally, we detected changes in jasmonic acid signaling and protein ubiquitination related genes, which have been implicated in DT more recently (Djilianov *et al.*, 2013; Liu *et al.*, 2018). In general, these findings indicate that *M. inflexa* shares some mechanistic components with highly DT plants. However, some of these may be common responses to drought, which are shared with DS plants (Pardo *et al.*, 2020).

This work also identifies notable differences between *M. inflexa* and highly DT plants. We observed an overall lack of fine-scale temporal coordination throughout the dehydration–rehydration time-course. We speculate that this derives from genotypic variability, an overall low-level response to dehydration, constitutive expression of some DhT transcripts, or the sequestration of transcripts in ribonucleoprotein particles prior to drying. Genotype-specific expression could easily obscure temporal patterns and has rarely been accounted for in studies of DT plants. That being said, it is also possible that *M. inflexa* simply does not exhibit a highly organized response to dehydration, which may contribute to its reduced tolerance relative to other bryophytes studied to date. We detected evidence of constitutive expression for some ELIPs and LEA

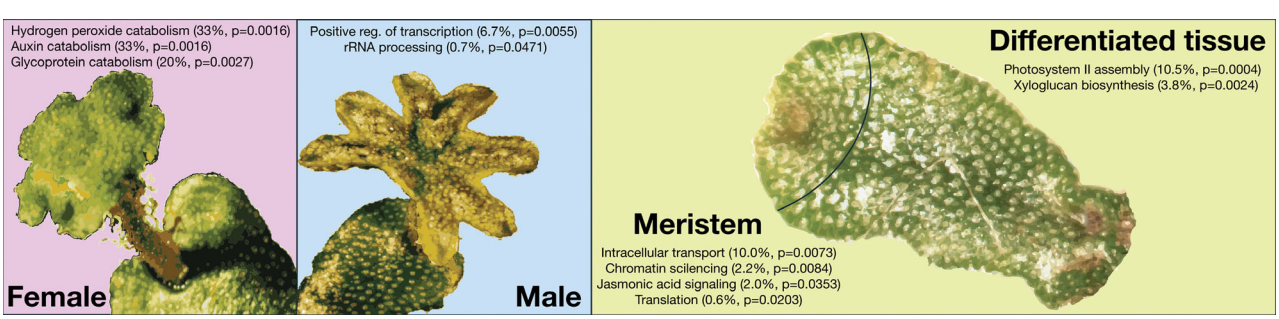

Figure 7. Summary of sex and tissue differences possibly contributing to differences in relative dehydration tolerance (DhT).
Based on gene ontology (GO) enrichment analyses of sex- and tissue-specific response, we constructed a general model to summarize differences in DhT among these samples. The percentage of genes that were differentially expressed for each GO term and statistical significance of enrichment is given.

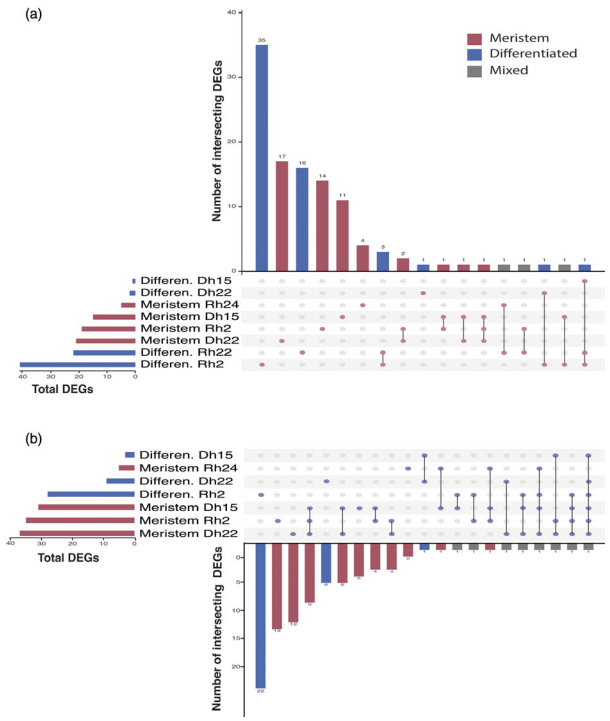

Figure 8. Upset plots showing the number of differentially expressed genes (DEGs) in each tissue and time-point for upregulated genes (a), and downregulated genes (b).
DEGs [false discovery rate (FDR) $P < 0.05$] were identified by comparing gene expression at experimental time-points with gene expression at baseline conditions to generate a tissue- and time-specific gene set. The total number of DEGs identified for each gene set is listed on the side bar plot, and the number of unique and common (non-overlapping and overlapping) genes is displayed in the main histogram. A colored circle indicates the gene set. Colored circles connected by a line indicate common (overlapping) gene sets. A gray circle indicates that the gene set is absent in that sample. There were no differentiated DEGs at Rh24. Bar color indicates tissue type.

proteins, but induced expression for others. In our previous work, we identified similar patterns for other DhT-related transcripts (Marks *et al.*, 2019b). Taken together, this suggests that *M. inflexa* employs a mixed or intermediate strategy involving both constitutive and inducible gene expression programs. The sequestration of DT-related mRNAs in ribonucleoprotein particles has been observed in other bryophytes, and could also obscure gene expression responses (Wood and Oliver, 1999; Oliver *et al.*, 2004). Although we detect enriched GO terms related to ribonucleoprotein complex assembly, we did not isolate sequestered mRNAs so we cannot conclusively determine the extent of mRNA sequestration. Additional variation in gene expression may derive from unaccounted factors in the experimental design, such as interacting stresses, disease or microbiome interactions. Most of the variation in gene expression was accounted for on PC1 (likely representing a response to changing water status), but ~34% of the variation in gene expression was not accounted for and was functionally enriched for genes involved in a diverse range of biological processes, making it difficult to link them with specific factors in the study.

Sequencing of six diverse genetic lines allowed us to investigate nuanced intraspecific variation in DhT. We intentionally selected phenotypically diverse genotypes for inclusion in this study in order to investigate the molecular underpinnings of intraspecific variation in DhT. We detected measurable genetic distance between individual genotypes, which likely contributes to the complex patterns of gene expression observed. Interestingly, male and female genotypes did not co-segregate in our analyses of genotype relationships, possibly related to low gene content on *M. inflexa* U and V chromosomes coupled with low expression of sex-linked genes under dehydration conditions. Because we called single nucleotide polymorphisms (SNPs) from RNA-seq data, this could cause any sex-specific signal to be diluted by the autosomal signal. Gene expression was also highly variable among genotypes, suggesting that dehydration programs are flexible. Importantly, these different programs are sufficient for minimizing damage from dehydration (to a point), and all genotypes generally survive.

Although plants generally survive dehydration, some tissue senescence is common. This study included plants collected from a single site in Trinidad in which females have consistently higher DhT than males (Marks *et al.*, 2016). Consequently, we expected to see distinct patterns of gene expression in response to dehydration between these two groups. Although we detected sexually dimorphic gene expression, the connection to differences in DhT is unclear. We suspect that much of the sex-specific gene expression observed here is related to secondary sexual dimorphisms that are established before dehydration (or sex-specific allocation to other functions that tradeoff with DhT). We detected differences among male and female plants under baseline conditions, supporting the idea that inherent differences among the sexes exist. Analyses of gene expression throughout the dehydration time-course revealed higher expression of transcription and rRNA processing genes in males, and increased ROS scavenging and catabolism in females (Figure 7). Males also exhibited expression of photosynthetic and biosynthetic genes at later stages of dehydration, which may trade off with mobilizing cellular protection programs. Studies of other DT plants suggest that early termination of photosynthetic processes can increase survival by minimizing photooxidative damage (Dinakar and Bartels, 2012).

Differences in survival related to tissue age have been documented in multiple DT plants (Blomstedt *et al.*, 2018; Radermacher *et al.*, 2019), and our findings add to the growing body of work showing that younger tissues are more resilient to dehydration. Analyses of gene expression in the meristematic and differentiated tissues of *M. inflexa*

revealed that meristems were enriched for GO terms related to intracellular transport and signaling, whereas the differentiated tissues were enriched for GO terms related to photosynthesis. Variation in cell wall characteristics may also contribute to relative differences in DhT between the meristematic and differentiated tissues.

In conclusion, we present a dehydration–rehydration transcriptome for the DhT liverwort, *M. inflexa*. Sequencing of multiple diverse genotypes allowed for detailed investigation of intraspecific variability in DhT. We identified some similarities between *M. inflexa* and highly DT plants, but also detected some noteworthy differences. Similar to highly tolerant DT plants, *M. inflexa* plants exhibited major changes in metabolism during drying and expression of DT-related proteins in the LEA and ELIP families. However, there was very little temporal synchronization of these processes across genotypes of *M. inflexa*, possibly related to complex patterns of genetic diversity or overall weak response to the stress of dehydration. We detected substantial variation in gene expression among genotypes and tissues under dehydration conditions, which underscores the complexity of DhT and highlights the need for comparative studies that seek to explore variation in and identify the core components of DT.

EXPERIMENTAL PROCEDURES

Study organism and genotype characteristics

Marchantia inflexa is a tropical liverwort with unisexual individuals that can reproduce sexually (via spores) or asexually via vegetative fragmentation or the production of specialized asexual propagules called gemmae. Plants grow as a dichotomously branching thallus with dorsiventral organization, and the haploid gametophyte is the dominant life stage. *Marchantia inflexa* typically grows along streams in tropical forests, but can also colonize more disturbed sites along roads. *Marchantia inflexa* is highly variable and exhibits sexual dimorphisms in DhT (Stieha *et al.*, 2014; Marks *et al.*, 2016, 2019a), growth rate, asexual reproduction (McLetchie and Puterbaugh, 2000; Brzyski *et al.*, 2014), response to exposure (Groen *et al.*, 2010a,b) and substitution rates of sex-specific genes (Marks *et al.*, 2019b).

Plants for the current study were collected in 2009 from a natural population along East Turure River (10°41′22.7″N 61°09′37.6″W) in Trinidad, The Republic of Trinidad and Tobago. Specimens were vouchered at the Missouri Botanical Garden (St Louis, MO, USA; specimen numbers M092113 and M092115) and at the National Herbarium of the Republic of Trinidad and Tobago (St Augustine, Trinidad; specimen number TRIN34616, D. N. McLetchie, collector). Plants were transported to the University of Kentucky, and the genetic uniqueness of each isolate was confirmed by microsatellite analyses (Brzyski *et al.*, 2014). Multiple clones of each genotype were propagated via vegetative fragmentation, watered daily, covered with 15% shade cloth and maintained in a climate-controlled greenhouse for ~8 years. For the current study, six unique genotypes with phenotypic differences in DhT were selected. These included the three most DhT genotypes (2×, 3× and 4×) and the three least DhT genotypes [1, 2, 8 years (previously called 8× but renamed as 8 years here for readability)] from the East Turure population (Marks *et al.*, 2016). Because there is a sex difference in DhT within the East Turure population, the three most DhT genotypes were females and the three least DhT genotypes were male, which provided an opportunity to link our findings to the previously characterized sexual dimorphism in DhT. In this paper, we generally refer to the high DhT group as 'female', and low DhT group as 'male'.

Dehydration treatment, tissue collection and RNA extraction

In addition to the description here, our sampling approach is presented in Figure S1 online. Plants were subjected to dehydration treatment as described in Marks *et al.* (2016). Briefly, thalli (~5 × 7 mm) were harvested from greenhouse-cultivated plants, fully hydrated for 24 h, and placed into dehydration chambers with an internal relative humidity (RH) of 75%. Air circulation was maintained by inserting a small fan in the chamber, and RH was verified with a HOBO™ RH sensor attached to a data logger (Onset Computer Corporation, Bourne, MA, USA). Each desiccation chamber contained 18 samples (three thalli from each of the six genotypes), which were randomized and placed into unlidded Petri dishes in the dehydration chamber. The chamber was maintained at 14°C, plants were dehydrated over the course of 22 h, then rehydrated with dH_2O, and maintained at 14°C for an additional 2 weeks. All dehydration assays were initiated at 14:00 hours (7.5 h after the lights came on) to reduce off target variation due to circadian rhythms.

Plants were sampled at five predetermined time-points during the dehydration–rehydration process: fully hydrated (baseline); partially dehydrated at 15 h (Dh15); dehydrated at 22 h (Dh22); 2 h after rehydration (Rh2); and 24 h after rehydration (Rh24). These time-points were selected based on the expected relative water content of plants at these times. Using data from previous studies conducted with the same genotypes cultivated under identical conditions, we estimate that sample relative water content is 100% at baseline, ~30–40% at Dh15, ~15–25% at Dh22, and 100% for both Rh2 and Rh24 (Marks *et al.*, 2016). Dehydration chambers were replicated three times per time-point for a total of 15 independent dehydration chambers. Because of technical difficulties, an additional assay was performed for time-point Rh24, bringing the total number of chambers to 16. At each time-point, samples were removed from the desiccation chamber and dissected into meristematic versus differentiated tissues using a 4-mm sterile biopsy punch. Samples were immediately flash-frozen in liquid nitrogen to prevent further transcriptional changes, RNA was extracted from three pooled samples of each tissue type for each genotype using the Triazol® Reagent according to the manufacturer's instructions, and stored at −80°C until needed (Figure S1).

To verify that dehydration assays were performing as expected, two randomly selected thalli from each assay were removed, and their recovery was quantified by measuring chlorophyll fluorescence 2 weeks after rehydration (when plants we expected to be fully recovered). For those genotypes the RNA extraction included two, not three thalli. We measured F_v/F_m of dark-adapted tissues (Krause and Weis, 1984) with an OS5-FL modulated chlorophyll fluorometer (Opti-Sciences, Tyngsboro, Massachusetts, USA). F_v/F_m is a measure of the maximum potential quantum efficiency of PSII, and is frequently used in studies of bryophyte DT to estimate recovery after a drying event (Marschall and Proctor, 1999; Proctor *et al.*, 2007; Bader *et al.*, 2013; Hájek and Vicherová, 2014). Measurement parameters were set to a saturation intensity of 100 (4000 μmol m^{-2} sec^{-1}) and a pulse duration of 0.8 sec. Gain and modulation were adjusted to achieve an adequate signal per manufacturer's directions.

To verify suspected differences in DhT among the meristematic and differentiated tissues, we conducted a separate experiment in which we subjected thalli ($n = 33$) to the dehydration assay (as described above), and documented the proportion and location of recovered versus necrotic tissues using ImageJ (Schneider *et al.*, 2012). Tissue survival was visually determined on the basis of green versus brown tissues. Samples were characterized 2 weeks after rehydration because tissue condition is most visually apparent at this stage.

Library preparation, sequencing and preassembly read processing

The RNA extraction with the highest RNA integrity number for each genotype × tissue × time-point was targeted for downstream library preparation. All samples were randomized during library preparation and sequencing to minimize batch effects. A total of 60 RNAseq libraries (meristematic and differentiated tissues from six unique genotypes at five time-points) were prepared for sequencing following the protocol described in Hunt (2015). Briefly, mRNA was isolated via poly(A) enrichment with the NEBNext® Poly(A) mRNA Magnetic Isolation Module, heat fragmented at 95°C for 2 min, and barcodes were integrated during first-strand cDNA syntheses with random primers ACACTCTTTCCCTACACGACGCTCTTCCGATCTNXXXNNNNNN (unique barcodes replaced XXX). A strand switching primer CGGTCTCGGCATTCCTGCTGAACCGCTCTTCCGATCTGG+G ('+G' denotes a locked nucleic acid) was used for second strand cDNA synthesis, which generated stranded libraries in a reverse-forward (RF) format. Libraries were size selected using Magbio HighPrep™ beads for a target fragment length of ~500 base pairs (bp) and enriched by 18 polymerase chain reaction cycles (primers: AATGATACGGCGACCACCGAGATCTACACTCTTTCCCTACACGACGCTCTTCCGATCT and CAAGCAGAAGACGGCATACGAGATCGGTCTCGGCATTCCTGCTGAACCGCTCTTCCGATCT). Library concentration was assessed with a Qubit dsDNA High Sensitivity Assay Kit, and fragment size was measured with a Bioanalyzer High Sensitivity DNA chip. Libraries were pooled in equal concentration and sequenced on four Illumina HiSeq4000 lanes for 150-bp paired-end reads at the University of California Davis Genome Center. The resulting sequence reads were demultiplexed with Sabre v1.000, quality assessed using FastQC (v0.11.2), and trimmed with Trimmomatic (v0.30_2) to remove adapter sequences and low-quality reads.

Transcriptome assembly, refinement and quality assessment

All sequence reads were pooled and assembled with Trinity (v2.6.6) following the genome guided pipeline (Schneider *et al.*, 2003). Briefly, RNAseq reads were aligned to the *M. inflexa* draft genome assembly (Marks *et al.*, 2019b) using Bowtie2 (v2-2.3.4.1) with default parameters (Langmead *et al.*, 2009). Reads that did not map to the *M. inflexa* genome (43%) appeared to derive primarily from fungal sources and were removed prior to assembly. Transcriptome assembly with Trinity (v2.6.6) specified options for genome guided assembly, RF library format, and a maximum intron length of 10 000 bp. Our initial assembly consisted of 50 135 468 assembled bp distributed across 93 958 transcripts with an N50 of 693 bp. Given that the large number of assembled transcripts suggests redundancy in the assembly, we eliminated poorly supported transcripts by filtering out those with a cumulative TMM < 1. This resulted in the removal of 66 961 transcripts and generated a filtered transcriptome consisting of 26 977 transcripts, which was used for all subsequent analyses. Four samples (meristematic tissues from genotypes 8 years, 2 years, and 3× at Rh24, and meristematic tissue from genotype 2 years at Rh2) were dropped because they had read counts below a threshold of three million reads. To estimate assembly completeness, we quantified the percentage of Universal Single-Copy Orthologs from the core eukaryota gene set of OrthoDB v9 of BUSCO v3 (Simão *et al.*, 2015) that were present in this *M. inflexa* transcriptome assembly.

Functional annotation

Marchantia inflexa transcripts were annotated using the Trinotate annotation pipeline (Haas *et al.*, 2013). Initially, transdecoder (https://github.com/TransDecoder) was used to identify protein coding regions for each *M. inflexa* transcript, HMMER (Eddy, 2011) was implemented to define Pfam protein domains (Finn *et al.*, 2014), and BLAST+ (Altschul *et al.*, 1990) was utilized for homology searches against UniProtKB/Swiss-Prot, and *A. thaliana* (Initiative, 2000), *P. patens* (Rensing *et al.*, 2008) and *M. polymorpha* (Bowman *et al.*, 2017; genomic data were downloaded from phytozome; Goodstein *et al.*, 2012). GO terms were associated with each *M. inflexa* transcript based on BLASTX homology searches, and all annotation information was integrated with SQLite (https://www.sqlite.org) to generate a combined annotation report. To summarize general patterns of gene function, we identified the most common GO terms and protein classes across the entire *M. inflexa* transcriptome with REVIGO (Supek *et al.*, 2011) and PANTHER (Mi *et al.*, 2017), respectively.

Genotype and sample relationships

To characterize genotype relationships, we identified all SNPs in our data, and estimated the genetic distance between each of the six genotypes included in this study. Initially, we generated genotype-specific alignments by mapping reads for each individual genotype to the *M. inflexa* draft genome using Bowtie2 (v2-2.3.4.1). To compute the genetic distance (proportion of loci that differ) among genotypes, we implemented samtools mpileup (v1.9) with default parameters and bcftools call (v1.9) to generate a vcf file with the --variants-only option specified. The resulting vcf file was filtered with vcftools (0.1.16) specifying options --recode, --max-missing-count 0.75, --max-alleles 2, and --min-alleles 2. The resulting VCF file included only binary SNPs that were present in at least 75% of the genotypes. These data were analyzed with the R package vcfR (Knaus and Grünwald, 2017) to compute genetic distance among samples.

RSEM (v1.3.0) (Li and Dewey, 2011) was implemented to calculate gene expression for each sample throughout the time-course. The resulting TMM normalized gene expression values were analyzed via PCA using the Trinity script PtR.pl to visualize sample relationships. Gene expression data were log2 transformed prior to PCA, and the 4163 transcripts with a cumulative TMM < 10 were excluded prior to clustering (Haas *et al.*, 2013). To determine the functional roles of genes contributing to PC1, the most enriched GO terms were identified for the 555 transcripts with loading scores > 1, and the 13 414 transcripts with loading scores < −1 via GO enrichment analyses with the R package topGO (Rahnenfuhrer, 2019). GO analyses were also conducted for genes with loading scores between 0.9 and −0.9 on PC1. PCA was conducted for each individual genotype, in an effort to parse out the effect of genotypic variation on total gene expression.

Changes in gene expression over time

To define DEGs, we implemented edgeR (Robinson *et al.*, 2010) using the Trinity script run_DE_analysis.pl. Gene count data were

normalized within edgeR. Initially, we targeted genes that were significantly up- or downregulated at each experimental time-point (Dh15, Dh22, Rh2, Rh24) relative to baseline conditions. From these analyses, we generated a set of non-redundant DEGs that were differentially expressed (with a FDR $P < 0.05$) relative to baseline conditions in at least one time-point.

We summarized gene expression dynamics throughout the dehydration–rehydration time-course via hierarchical clustering analyses of log2-transformed, median-centered TMM values for all non-redundant DEGs in JMP12 (SAS Institute, Cary, NC, USA). DEGs were clustered into seven semi-distinct groups based on similarity in expression patterns, and the most enriched GO terms for each cluster were identified. To gain further insight into temporal changes in gene expression, we tracked DEGs throughout the dehydration–rehydration time-course. To do so, we assigned each transcript to a group based on their expression value (up, down or not DE) at each time-point, and generated an alluvial diagram with the R package alluvial (Edwards and Bojanowski, 2016). We summarized the function of genes showing characteristic expression patterns (upregulated across all experimental time-points, downregulated at all experimental time-points, and dehydration- or rehydration-specific expression) via GO enrichment analysis.

We conducted targeted analyses to characterize changes in LEA and ELIP expression throughout the dehydration–rehydration process. *Marchantia inflexa* LEAs and ELIPs were identified via HMM and TBLASTX searches. HMMs for each of the eight LEA families (LEAs 1–6, dehydrins and seed maturation proteins) were obtained from the PFAM database (http://pfam.xfam.org), and used to generate a searchable HMM profile using HMMER3.0 (Wheeler and Eddy, 2013). The program hmmseach was used to identify homologous *M. inflexa* sequences, and TMM gene expression values for each *M. inflexa* ortholog were extracted from the gene expression matrix. ELIPs were identified via homology with the *M. polymorpha* ELIPs listed in Vanburen *et al.* (2019). Homology between *M. polymorpha* and *M. inflexa* has been previously characterized (Marks *et al.*, 2019b), so we simply extracted the *M. inflexa* orthologs to each *M. polymorpha* ELIP. Again, all LEA and ELIPs with a cumulative TMM < 10 were removed from analyses, and the expression levels of the remaining transcripts were plotted as a heatmap to visualize sample relationships and gene expression patterns using JMP12. Relatedness of LEA subfamilies and ELIPs was determined through analyses of sequence similarity. The *M. inflexa* translated coding sequences for each putative LEA and ELIP were aligned with Clustal Omega (Sievers *et al.*, 2011) and visualized as a cladogram.

Intraspecific variation in DhT

To characterize intraspecific variation in gene expression during dehydration and rehydration, we identified genes that were differentially expressed over time in the high DhT group (females), low DhT group (males), meristematic and differentiated tissues. To do so, we compared gene expression at experimental time-points with gene expression at baseline conditions for each group and tissue individually. These DEGs were visualized with UpSetR (Conway *et al.*, 2017), to identify unique versus shared DEGs. GO analyses were implemented to gain insight into the functional roles of sex- and tissue-specific expression dynamics.

ACKNOWLEDGEMENTS

This work was funded by Kentucky Science and Engineering Foundation's Research and Development Excellence grant to DNM (KSEF-148-502-16-372), the University of Kentucky Department of Biology Ribble Endowment Graduate Fellowship to RAM, the American Bryological and Lichenological Society Anderson and Crum Bryology Research Award to RAM, and the Karri Casner Environmental Sciences Fellowship to RAM. This work would not have been possible without access to critical facilities provided by the University of Kentucky, College of Agriculture, Food and Environment (greenhouse space); the Wildlife Section, Forestry Division, Ministry of Agriculture Land and Marine Resources of Trinidad and Tobago (collection and export permits); the Water and Sewage Authority (access to the field research sites). The authors thank Drs Arthur Hunt, Manohar Chakrabarti and Mel Oliver for their assistance with library preparation; Oliva Boughey for piloting RNA extraction methodologies; and Drs Carol Baskin, Michael Goodin, Daniel Herring, and two anonymous reviewers for helpful comments and discussions that improved the rigor and presentation of this work.

AUTHOR CONTRIBUTIONS

RAM and DNM conceived of the study. RAM conduced all experiments and prepared samples for sequencing. All authors contributed to data analyses and interpretation. RAM wrote the manuscript. All authors reviewed and edited the manuscript.

CONFLICTS OF INTEREST

The authors have no conflicts of interest to declare.

DATA AVAILABILITY STATEMENT

The data associated with this study have been deposited in NCBI under the BioProject number PRJNA577280 and SRA accession numbers SRX6984587-642. The assembled transcriptome, coding and peptide sequences are available on figshare (https://doi.org/10.6084/m9.figshare.12461756.v1).

SUPPORTING INFORMATION

Additional Supporting Information may be found in the online version of this article.

Figure S1. Schematic of experimental design.

Figure S2. Mean F_v/F_m and percent tissue recovery from dehydration treatment.

Figure S3. Clustered dendrogram of sample relationships computed.

Figure S4. PCA of global gene expression for each individual genotype.

REFERENCES

Alpert, P. (2005) Sharing the secrets of life without water. *Integr. Comp. Biol.* **45**, 683–684.

Alpert, P. and Oliver, M.J. (2002) Drying Without Dying. In *Desiccation and Survival in Plants: Drying Without Dying* (Black, M. and Pritchard, H. W., eds). New York, NY: CABI Publishing.

Altschul, S.F., Gish, W., Miller, W., Myers, E.W. and Lipman, D.J. (1990) Basic local alignment search tool. *J. Mol. Biol.* **215**, 403–410.

Artur, M.A.S., Zhao, T., Ligterink, W., Schranz, M.E. and Hilhorst, H.W.M. (2019) Dissecting the genomic diversification of *LATE EMBRYOGENESIS ABUNDANT (LEA)* protein gene families in plants. *Genome Biol. Evol* **11**, 459–471.

Bader, M.Y., Reich, T., Wagner, S., González González, A.S. and Zotz, G. (2013) Differences in desiccation tolerance do not explain altitudinal distribution patterns of tropical bryophytes. *J. Bryol.* **35**, 47–56.

Bischler, H. (1984) *Marchantia L: The New World Species (Bryophytorum Bibliotheca, Band 26).* Port Jervis, NY: Lubrecht & Cramer Ltd.

Blomstedt, C.K., Griffiths, C.A., Gaff, D.F., Hamill, J.D. and Neale, A.D. (2018) Plant desiccation tolerance and its regulation in the foliage of resurrection "flowering-plant" species. *Agronomy*, **8**, 146.

Bowman, J.L., Kohchi, T., Yamato, K.T. *et al.* (2017) Insights into land plant evolution garnered from the *Marchantia polymorpha* genome. *Cell*, **171**, 287–304.e15.

Bremer, A., Wolff, M., Thalhammer, A. and Hincha, D.K. (2017) Folding of intrinsically disordered plant LEA proteins is driven by glycerol-induced crowding and the presence of membranes. *FEBS J.* **284**, 919–936.

Brzyski, J.R., Taylor, W. and McLetchie, D.N. (2014) Reproductive allocation between the sexes, across natural and novel habitats, and its impact on genetic diversity. *Evol. Ecol.* **28**, 247–261.

Choudhury, F.K., Rivero, R.M., Blumwald, E. and Mittler, R. (2017) Reactive oxygen species, abiotic stress and stress combination. *Plant J.* **90**, 856–867.

Conway, J.R., Lex, A. and Gehlenborg, N. (2017) UpSetR: an R package for the visualization of intersecting sets and their properties. *Bioinformatics*, **33**, 2938–2940.

Costa, M.-C.-D., Artur, M.A.S., Maia, J. *et al.* (2017) A footprint of desiccation tolerance in the genome of *Xerophyta viscosa*. *Nat. Plants*, **3**, 17038.

Crowe, J.H., Carpenter, J.F. and Crowe, L.M. (1998) The role of vitrification in anhydrobiosis. *Annu. Rev. Physiol.* **60**, 73–103.

Dai, A. (2013) Increasing drought under global warming in observations and models. *Nat. Clim. Change*, **3**, 52–58.

Dinakar, C. and Bartels, D. (2012) Light response, oxidative stress management and nucleic acid stability in closely related Linderniaceae species differing in desiccation tolerance. *Planta*, **236**, 541–555.

Dinakar, C. and Bartels, D. (2013) Desiccation tolerance in resurrection plants: new insights from transcriptome, proteome and metabolome analysis. *Front. Plant Sci.* **4**, 482.

Dinakar, C., Djilianov, D. and Bartels, D. (2012) Photosynthesis in desiccation tolerant plants: Energy metabolism and antioxidative stress defense. *Plant Sci.* **182**, 29–41.

Djilianov, D.L., Dobrev, P.I., Moyankova, D.P., Vankova, R., Georgieva, D.T., Gajdošová, S. and Motyka, V. (2013) Dynamics of endogenous phytohormones during desiccation and recovery of the resurrection plant species *Haberlea rhodopensis*. *J. Plant Growth Regul.* **32**, 564–574.

Eddy, S.R. (2011) Accelerated profile HMM searches. *PLoS Comput. Biol.* **7**, e1002195.

Edwards, R. and Bojanowski, M. (2016) alluvial: R package for creating alluvial diagramsion info. R package version: 0.1-2. Available from: https://github.com/mbojan/alluvial.

Farrant, J.M. (2000) A comparison of mechanisms of desiccation tolerance among three angiosperm resurrection plant species. *Plant Ecol.* **151**, 29–39.

Farrant, J.M. and Kruger, L.A. (2001) Longevity of dry *Myrothamnus flabellifolius* in simulated field conditions. *Plant Growth Regul.* **35**, 109–120.

Farrant, J.M., Lehner, A., Cooper, K. and Wiswedel, S. (2009) Desiccation tolerance in the vegetative tissues of the fern *Mohria caffrorum* is seasonally regulated. *Plant J.* **57**, 65–79.

Finn, R.D., Bateman, A., Clements, J. *et al.* (2014) Pfam: the protein families database. *Nucleic Acids Res.* **42**, D222–D230.

Ghasempour, H.R., Gaff, D.F., Williams, R.P.W. and Gianello, R.D. (1998) Contents of sugars in leaves of drying desiccation tolerant flowering plants, particularly grasses. *Plant Growth Regul.* **24**, 185–191.

Goodstein, D.M., Shu, S., Howson, R. *et al.* (2012) Phytozome: a comparative platform for green plant genomics. *Nucleic Acids Res.* **40**, D1178–D1186.

Greenwood, J.L., Stark, L.R. and Chiquoine, L.P. (2019) Effects of rate of drying, life history phase, and ecotype on the ability of the moss *Bryum argenteum* to survive desiccation events and the influence on conservation and selection of material for restoration. *Front. Ecol. Evol.* **7**, 388.

Groen, K.E., Stieha, C.R., Crowley, P.H. and McLetchie, D.N. (2010a) Sex-specific plant responses to light intensity and canopy openness: implications for spatial segregation of the sexes. *Oecologia*, **162**, 561–570.

Groen, K.E., Stieha, C.R., Crowley, P.H. and McLetchie, D.N. (2010b) Sex-specific plant responses to two light levels in the liverwort *Marchantia inflexa* (Marchantiaceae). *Bryologist*, **113**, 81–89.

Haas, B.J., Papanicolaou, A., Yassour, M. *et al.* (2013) De novo transcript sequence reconstruction from RNA-seq using the Trinity platform for reference generation and analysis. *Nat. Protoc.* **8**, 1494–1512.

Hájek, T. and Vicherová, E. (2014) Desiccation tolerance of *Sphagnum* revisited: a puzzle resolved. *Plant Biol.* **16**, 765–773.

Hunt, A.G. (2015) A rapid, simple, and inexpensive method for the preparation of strand-specific RNA-Seq Libraries. *Methods Mol. Biol.* **1255**, 195–207.

Illing, N., Denby, K.J., Collett, H., Shen, A. and Farrant, J.M. (2005) The signature of seeds in resurrection plants: a molecular and physiological comparison of desiccation tolerance in seeds and vegetative tissues. *Integr. Comp. Biol.* **45**, 771–787.

Arabidopsis Genome Initiative. (2000) Analysis of the genome sequence of the flowering plant *Arabidopsis thaliana*. *Nature*, **408**, 796–815.

Juvany, M. and Munné-Bosch, S. (2015) Sex-related differences in stress tolerance in dioecious plants: a critical appraisal in a physiological context. *J. Exp. Bot.* **66**, 6083–6092.

Knaus, B.J. and Grünwald, N.J. (2017) vcfr: a package to manipulate and visualize variant call format data in R. *Mol. Ecol. Resour.* **17**, 44–53.

Krause, G.H. and Weis, E. (1984) Chlorophyll fluorescence as a tool in plant physiology: II. Interpretation of fluorescence signals. *Photosynth. Res.* **5**, 139–157.

Langmead, B., Trapnell, C., Pop, M. and Salzberg, S.L. (2009) Ultrafast and memory-efficient alignment of short DNA sequences to the human genome. *Genome Biol.* **10**, R25.

Lesk, C., Rowhani, P. and Ramankutty, N. (2016) Influence of extreme weather disasters on global crop production. *Nature*, **529**, 84–87.

Li, B. and Dewey, C.N. (2011) RSEM: accurate transcript quantification from RNA-Seq data with or without a reference genome. *BMC Bioinformatics*, **12**, 323.

Lin, C.-T., Xu, T., Xing, S.-L., Zhao, L., Sun, R.-Z., Liu, Y., Moore, J.P. and Deng, X. (2019) Weighted gene co-expression network analysis (WGCNA) reveals the hub role of protein ubiquitination in the acquisition of desiccation tolerance in *Boea hygrometrica*. *Plant Cell Physiol.* **60**, 2707–2719.

Liu, J., Moyankova, D., Lin, C.T., Mladenov, P., Sun, R.Z., Djilianov, D. and Deng, X. (2018) Transcriptome reprogramming during severe dehydration contributes to physiological and metabolic changes in the resurrection plant *Haberlea rhodopensis*. *BMC Plant Biol.* **18**, 351.

Liu, X., Wang, Z., Wang, L., Wu, R., Phillips, J. and Deng, X. (2009) LEA 4 group genes from the resurrection plant *Boea hygrometrica* confer dehydration tolerance in transgenic tobacco. *Plant Sci.* **176**, 90–98.

Marks, R.A., Burton, J.F. and McLetchie, D.N. (2016) Sex differences and plasticity in dehydration tolerance: insight from a tropical liverwort. *Ann. Bot.* **118**, 347–356.

Marks, R.A., Pike, B.D. and Nicholas, M.D. (2019a) Water stress tolerance tracks environmental exposure and exhibits a fluctuating sexual dimorphism in a tropical liverwort. *Oecologia*, **191**, 791–802.

Marks, R.A., Smith, J.J., Cronk, Q., Grassa, C.J. and McLetchie, D.N. (2019b) Genome of the tropical plant *Marchantia inflexa*: implications for sex chromosome evolution and dehydration tolerance. *Sci. Rep.* **9**, 8722.

Marschall, M. and Proctor, M.C.F. (1999) Desiccation tolerance and recovery of the leafy liverwort *Porella platyphylla* (L.)Pfeiff.: chlorophyll-fluorescence measurements. *J. Bryol.* **21**, 257–262.

McLetchie, D.N. and Puterbaugh, M.N. (2000) Population sex ratios, sex-specific clonal traits and tradeoffs among these traits in the liverwort *Marchantia inflexa*. *Oikos*, **90**, 227–237.

Mi, H., Huang, X., Muruganujan, A., Tang, H., Mills, C., Kang, D. and Thomas, P.D. (2017) PANTHER version 11: expanded annotation data from gene ontology and reactome pathways, and data analysis tool enhancements. *Nucleic Acids Res.* **45**, D183–D189.

Moore, J.P., Nguema-Ona, E., Chevalier, L., Lindsey, G.G., Brandt, W.F., Lerouge, P., Farrant, J.M. and Driouich, A. (2006) Response of the leaf cell wall to desiccation in the resurrection plant *Myrothamnus flabellifolius*. *Plant Physiol.* **141**, 651–662.

Moore, J.P., Vicré-Gibouin, M., Farrant, J.M. and Driouich, A. (2008) Adaptations of higher plant cell walls to water loss: drought vs desiccation. *Physiol. Plant.* **134**, 237–245.

Oliver, M.J., Cushman, J.C. and Koster, K.L. (2010) Dehydration tolerance in plants. In *Plant Stress Tolerance* (Sunkar, R., ed). Totowa, New Jersey: Humana Press, pp. 3–24.

Oliver, M.J., Dowd, S.E., Zaragoza, J., Mauget, S.A. and Payton, P.R. (2004) The rehydration transcriptome of the desiccation-tolerant bryophyte *Tortula ruralis:* transcript classification and analysis. *BMC Genomics*, **5**, 89.

Oliver, M.J., Farrant, J.M., Hilhorst, H.W.M., Mundree, S., Williams, B. and Bewley, J.D. (2020) Desiccation tolerance: avoiding cellular damage during drying and rehydration. *Annu. Rev. Plant Biol.* **71**, 435–460.

Oliver, M.J., Guo, L., Alexander, D.C., Ryals, J.A., Wone, B.W.M. and Cushman, J.C. (2011) A sister group contrast using untargeted global metabolomic analysis delineates the biochemical regulation underlying desiccation tolerance in *Sporobolus stapfianus*. *Plant Cell*, **23**, 1231–1248.

Oliver, M.J., Mishler, B.D. and Quisenberry, J.E. (1993) Comparative measures of desiccation-tolerance in the *Tortula ruralis* complex. I. variation in damge control and repair. *Am. J. Bot.* **80**, 127–136.

Oliver, M.J., Tuba, Z. and Mishler, B.D. (2000) The evolution of vegetative desiccation tolerance in land plants. *Plant Ecol.* **151**, 85–100.

Pardo, J., Wai, C.M., Chay, H., Madden, C.F., Hilhorst, H.W.M., Farrant, J.M. and VanBuren, R. (2020) Intertwined signatures of desiccation and drought tolerance in grasses. *Proc. Natl Acad. Sci. USA*, **117**, 10079–10088.

Platt, K., Oliver, M.J. and Thomson, W.W. (1997). Importance of the fixative for reliable ultrastructural preservation of poikilohydric plant tissues. Observations on dry, partially, and fully hydrated tissues of *Selaginella*. *Ann. Bot.* **80**, 599–610.

Proctor, M.C.F., Oliver, M.J., Wood, A.J., Stark, L.R., Cleavitt, N.L. and Mishler, B.D. (2007) Desiccation-tolerance in bryophytes: a review. *Bryologist*, **110**, 595–621.

Proctor, M.C.F. and Pence, V.C. (2002) Vegetative tissues: bryophytes, vascular resurrection plants and vegetative propagules. In *Desiccation and Survival in Plants: Drying Without Dying* (Black, M. and Prichard, H. R., eds). Wallingford: CABI, 207–237.

Radermacher, A.L., du Toit, S.F. and Farrant, J.M. (2019) Desiccation-driven senescence in the resurrection plant *Xerophyta schlechteri* (Baker) N.L. Menezes: comparison of anatomical, ultrastructural, and metabolic responses between senescent and non-senescent tissues. *Front. Plant Sci.* **10**, 1396.

Rahnenfuhrer, A. (2019) topGO: Enrichment Analysis for Gene Ontology. R package version 2.40.0.

Rensing, S.A., Lang, D., Zimmer, A.D. *et al.* (2008) The *Physcomitrella* genome reveals evolutionary insights into the conquest of land by plants. *Science*, **319**, 64–69.

Robinson, M.D., McCarthy, D.J. and Smyth, G.K. (2010) edgeR: a Bioconductor package for differential expression analysis of digital gene expression data. *Bioinformatics*, **26**, 139–140.

Scheibe, R. and Beck, E. (2011) Drought, desiccation, and oxidative stress. In *Plant Desiccation Tolerance. Ecological Studies (Analysis and Synthesis)*(Lüttge, U., Beck, E. and Bartels, D., eds). Berlin, Heidelberg: Springer, pp. 209–231.

Schneider, H., Manz, B., Westhoff, M. *et al.* (2003) The impact of lipid distribution, composition and mobility on xylem water refilling of the resurrection plant *Myrothamnus flabellifolia*. *New Phytol.* **159**, 487–505.

Schneider, C.A., Rasband, W.S. and Eliceiri, K.W. (2012) NIH image to ImageJ: 25 years of image analysis. *Nat. Methods*, **9**, 671–675.

Sharma, P., Jha, A.B., Dubey, R.S. and Pessarakli, M. (2012) Reactive oxygen species, oxidative damage, and antioxidative defense mechanism in plants under stressful conditions. *J. Bot.* **2012**, 1–26.

Sievers, F., Wilm, A., Dineen, D. *et al.* (2011) Fast, scalable generation of high-quality protein multiple sequence alignments using Clustal Omega. *Mol. Syst. Biol.* **7**, 539.

Simão, F.A., Waterhouse, R.M., Ioannidis, P., Kriventseva, E.V. and Zdobnov, E.M. (2015) BUSCO: assessing genome assembly and annotation completeness with single-copy orthologs. *Bioinformatics*, **31**, 3210–3212.

Smirnoff, N. (1992) The carbohydrates of bryophytes in relation to desiccation tolerance. *J. Bryol.* **17**, 185–191.

Smith, J.J., Timoshevskaya, N., Ye, C. *et al.* (2018) The sea lamprey germline genome provides insights into programmed genome rearrangement and vertebrate evolution. *Nat. Genet.* **50**, 270–277.

Stark, L.R., Oliver, M.J., Mishler, B.D. and McLetchie, D.N. (2007) Generational differences in response to desiccation stress in the desert moss *Tortula inermis*. *Ann. Bot.* **99**, 53–60.

Stieha, C.R., Middleton, A.R., Stieha, J.K., Trott, S.H. and Mcletchie, D.N. (2014) The dispersal process of asexual propagules and the contribution to population persistence in *Marchantia* (Marchantiaceae). *Am. J. Bot.* **101**, 348–356.

Supek, F., Bošnjak, M., Škunca, N. and Šmuc, T. (2011) REVIGO summarizes and visualizes long lists of gene ontology terms. *PLoS One*, **6**, e21800.

Trenberth, K. (2011) Changes in precipitation with climate change. *Clim. Res.* **47**, 123–138.

Tuba, Z., Protor, C.F. and Csintalan, Z. (1998) Ecophysiological responses of homoiochlorophyllous and poikilochlorophyllous desiccation tolerant plants: a comparison and an ecological perspective. *Plant Growth Regul.* **24**, 211–217.

VanBuren, R., Man Wai, C., Pardo, J., Giarola, V., Ambrosini, S., Song, X. and Bartels, D. (2018) Desiccation tolerance evolved through gene duplication and network rewiring in *Lindernia*. *Plant Cell*, **30**, 2943–2958.

Vanburen, R., Pardo, J., Wai, C.M., Evans, S. and Bartels, D. (2019) Massive tandem proliferation of ELIPs supports convergent evolution of desiccation tolerance across land plants. *Plant Physiol. Prev.* **179**, 1040–1049.

Vicré, M., Farrant, J.M. and Driouich, A. (2004) Insights into the cellular mechanisms of desiccation tolerance among angiosperm resurrection plant species. *Plant Cell Environ.* **27**, 1329–1340.

Wheeler, T.J. and Eddy, S.R. (2013) nhmmer: DNA homology search with profile HMMs. *Bioinformatics*, **29**, 2487–2489.

Vander Willigen, C., Pammenter, N.W., Mundree, S. and Farrant, J. (2001) Some physiological comparisons between the resurrection grass, *Eragrostis nindensis*, and the related desiccation-sensitive species, E. curvula. *Plant Growth Regul.* **35**, 121–129.

Wood, A.J. and Oliver, M.J. (1999) Translational control in plant stress: the formation of messenger ribonucleoprotein particles (mRNPs) in response to desiccation of *Tortula ruralis* gametophytes. *Plant J.* **18**, 359–370.

Zeng, Q., Chen, X. and Wood, A.J. (2002) Two early light-inducible protein (ELIP) cDNAs from the resurrection plant *Tortula ruralis* are differentially expressed in response to desiccation, rehydration, salinity, and high light. *J. Exp. Bot.* **53**, 1197–1205.